A double-hexameric MCM2-7 complex is loaded onto origin DNA during licensing of eukaryotic DNA replication

Cecile Evrin, Pippa Clarke, Juergen Zech, Rudi Lurz, Jingchuan Sun, Stefan Uhle, Huilin Li, Bruce Stillman, and Christian Speck

Abstract

During pre-replication complex (pre-RC) formation, origin recognition complex (ORC), Cdc6, and Cdt1 cooperatively load the 6-subunit mini chromosome maintenance (MCM2-7) complex onto DNA. Loading of MCM2-7 is a prerequisite for DNA licensing that restricts DNA replication to once per cell cycle. During S phase MCM2-7 functions as part of the replicative helicase but within the pre-RC MCM2-7 is inactive. The organization of replicative DNA helicases before and after loading onto DNA has been studied in bacteria and viruses but not eukaryotes and is of major importance for understanding the MCM2-7 loading mechanism and replisome assembly. Lack of an efficient reconstituted pre-RC system has hindered the detailed mechanistic and structural analysis of MCM2-7 loading for a long time. We have reconstituted Saccharomyces cerevisiae pre-RC formation with purified proteins and showed efficient loading of MCM2-7 onto origin DNA in vitro. MCM2-7 loading was found to be dependent on the presence of all pre-RC proteins, origin DNA, and ATP hydrolysis. The quaternary structure of MCM2-7 changes during pre-RC formation: MCM2-7 before loading is a single hexamer in solution but is transformed into a double-hexamer during pre-RC formation. Using electron microscopy (EM), we observed that loaded MCM2-7 encircles DNA. The loaded MCM2-7 complex can slide on DNA, and sliding is not directional. Our results provide key insights into mechanisms of pre-RC formation and have important implications for understanding the role of the MCM2-7 in establishment of bidirectional replication forks.

DNA replication is a precisely ordered process that requires the stepwise assembly of the replication machinery (1). The sites of replication protein assembly occur on DNA replication origins or autonomous replicating sequences (ARS). In eukaryotic cells, origins are recognized by a conserved 6-protein origin recognition complex (ORC) (2). ORC is bound to DNA throughout the cell cycle and during late M/early G1 phase recruits the Cdc6 protein, which facilitates MCM2-7 loading (3–5). Cdt1 forms a complex with MCM2-7 during late M phase (6). Within the nucleus Cdt1 recruits MCM2-7 to the ORC-Cdc6-DNA complex via an interaction with Orc6 to form a prereplication complex (pre-RC) (5). Cdc6 ATP hydrolysis is required for MCM2-7 loading, and Orc1 ATP hydrolysis promotes the release of the MCM2-7 complex from ORC to finish the process of pre-RC formation and DNA licensing (7, 8). Although only 2 MCM2-7 hexamers are needed to establish bidirectional replication forks at an origin, between 10 and 20 MCM2-7 complexes are loaded onto each replication origin during G1 in animal cells (9). The additional loaded MCM2-7 complexes function to protect cells

from replicative stress (10, 11). Once the MCM2-7 complex is loaded onto DNA it becomes resistant to high salt, suggesting that it is physically linked to DNA (12). During the G1/S transition the pre-RC is remodeled to form the pre-initiation complex (pre-IC). Binding of pre-IC proteins and protein kinase activity stimulates MCM2-7 helicase activity (13). Pre-IC formation culminates in the recruitment of DNA polymerases and the start of active DNA replication (14).

ORC and Cdc6 belong to the AAA+ family of ATP binding proteins (4, 15), a family that commonly forms ring- or spiral-shaped structures. A spiral-shaped structure consisting of 5 AAA+ proteins within the replication factor C (RFC) complex functions to destabilize the homotrimeric proliferating cell nuclear antigen (PCNA) ring during PCNA loading onto DNA. In an analogous scenario it is possible that ORC-Cdc6 could destabilize the MCM2-7 ring. This would result in ring opening during the MCM2-7 loading reaction (4, 16).

MCM2-7 is the best candidate for the eukaryotic replicative helicase, because it can unwind DNA (17) and travels with the fork (18). However, MCM2-7 alone is a very weak helicase and requires further proteins (Cdc45 and GINS) or posttranslational modifications for full activity (17, 19). For a long time, analysis of MCM2-7's role in pre-RC formation and MCM2-7's helicase activity was hampered by the fact that MCM2-7 can form multiple complexes in vitro. MCM2-7 exists as MCM467, MCM35, MCM2-7, and other subcomplexes. Previous MCM2-7 purifications contained a mixture of different complexes varying in mass, ranging from single subunit monomers to very large aggregated complexes (17, 20, 21). Until now the structure of eukaryotic MCM2-7 before, during, and after loading remained poorly understood.

In this study we developed a purification method for MCM2-7 from yeast that enabled reconstitution of pre-RC formation in vitro. Parallel biochemical and EM approaches showed that MCM2-7, although a single hexamer in solution, forms a double hexamer that can slide on DNA after loading. These results have important implications for understanding how DNA is licensed and how replication forks are formed.

Results

Purification of a Single-Hexameric MCM2-7 Complex. Loading of MCM2-7 onto DNA during pre-RC formation is inhibited by B-type cyclin-dependent kinases (22). To obtain an MCM2-7 complex competent for pre-RC formation, we expressed MCM2-7 in yeast cells arrested in G1 phase when B-type cyclin-dependent kinases were inactive (Fig. 1A). We used an HA-tagged Mcm3 subunit to enrich for a population of MCM2-7 devoid of MCM467, a well-known contaminating subcomplex that has a similar size as MCM2-7 and has helicase activity (23). The HA affinity-purified material was then applied to a gel-filtration column to remove the smaller MCM35 subcomplex. The final MCM2-7 preparation was analyzed on a gel-filtration column and eluted in the same fraction as the 669-kDa marker protein (Fig. 1B). This fractionation result is consistent with the calculated molecular mass of

605 kDa for MCM2-7. A Coomassie Brilliant Blue–stained gel showed bands of equal intensity for all 6 MCM2-7 proteins (Fig. 1C). These data are consistent with the purification of a single heterohexameric MCM2-7 complex.

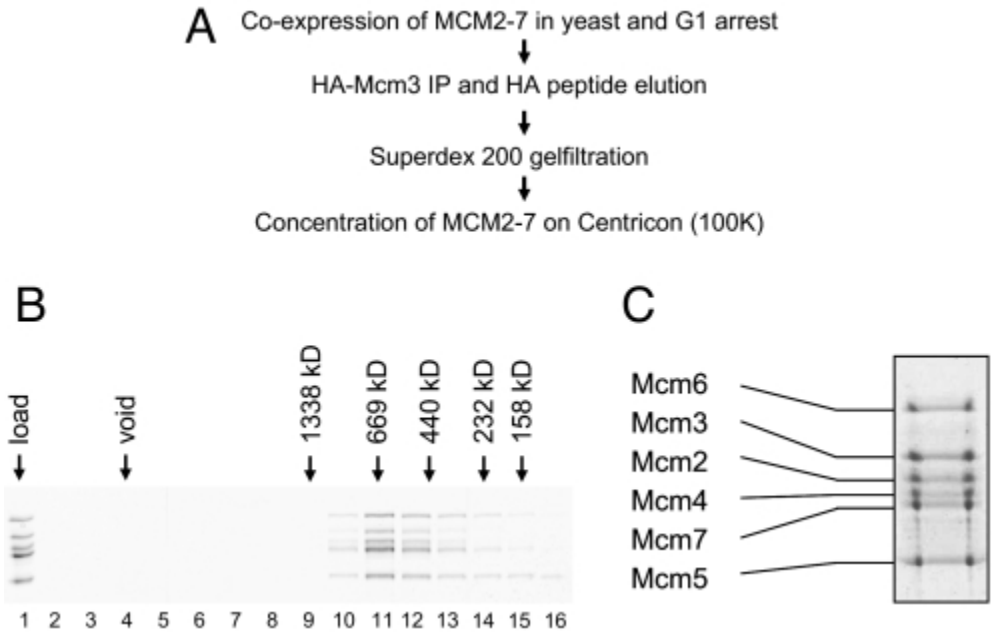

Figure 1 MCM2-7 purification and characterization. (*A*) Strategy for the expression and purification of MCM2-7. (*B*) Two micrograms of purified MCM2-7 was fractionated on a Superose 6 column. Arrows indicate fractionation of marker proteins (see *Materials and Methods*). Load (lane 1) and elution fractions (lanes 2–16) were separated by 7.5% SDS-PAGE and the proteins visualized by silver staining. MCM2-7 peaked at the 669-kDa marker (lane 11), which is consistent with their calculated mass of 605 kDa. (*C*) Purified MCM2-7 was separated on a 10% SDS-PAGE.

Reconstitution of Pre-RC Formation with Purified Proteins. In vitro assays for pre-RC assembly at Saccharomyces cerevisiae origins of replication have proven to be a useful tool to study the mechanism of pre-RC formation (7, 8, 24, 25). Previous assays used yeast extract and linear origin-containing DNA (7, 8, 24, 25); however, the assays were very inefficient in MCM2-7 loading, which hindered a structural characterization of the MCM2-7 complex before and after the loading. We used highly purified pre-RC proteins and circular origin-containing DNA. A plasmid containing the yeast origin ARS1 was cross-linked with biotin and subsequently immobilized on streptavidin-coated magnetic beads. Use of purified proteins allowed us to monitor pre-RC formation by silver staining of pre-RC components after elution of origin DNA bound complexes. To test our proteins for pre-RC formation activity we combined recombinant ORC, Cdc6, and Cdt1 with purified MCM2-7 and origin DNA (Fig. 2A). MCM2-7 binding to DNA was dependent on the presence of all proteins; removal of an individual protein from the reaction mixture did not support MCM2-7 binding (Fig. 2A, compare lanes 5–8 with lane 9). In the absence of DNA, no proteins were observed in the bound material (Fig. 2A, lane 4).

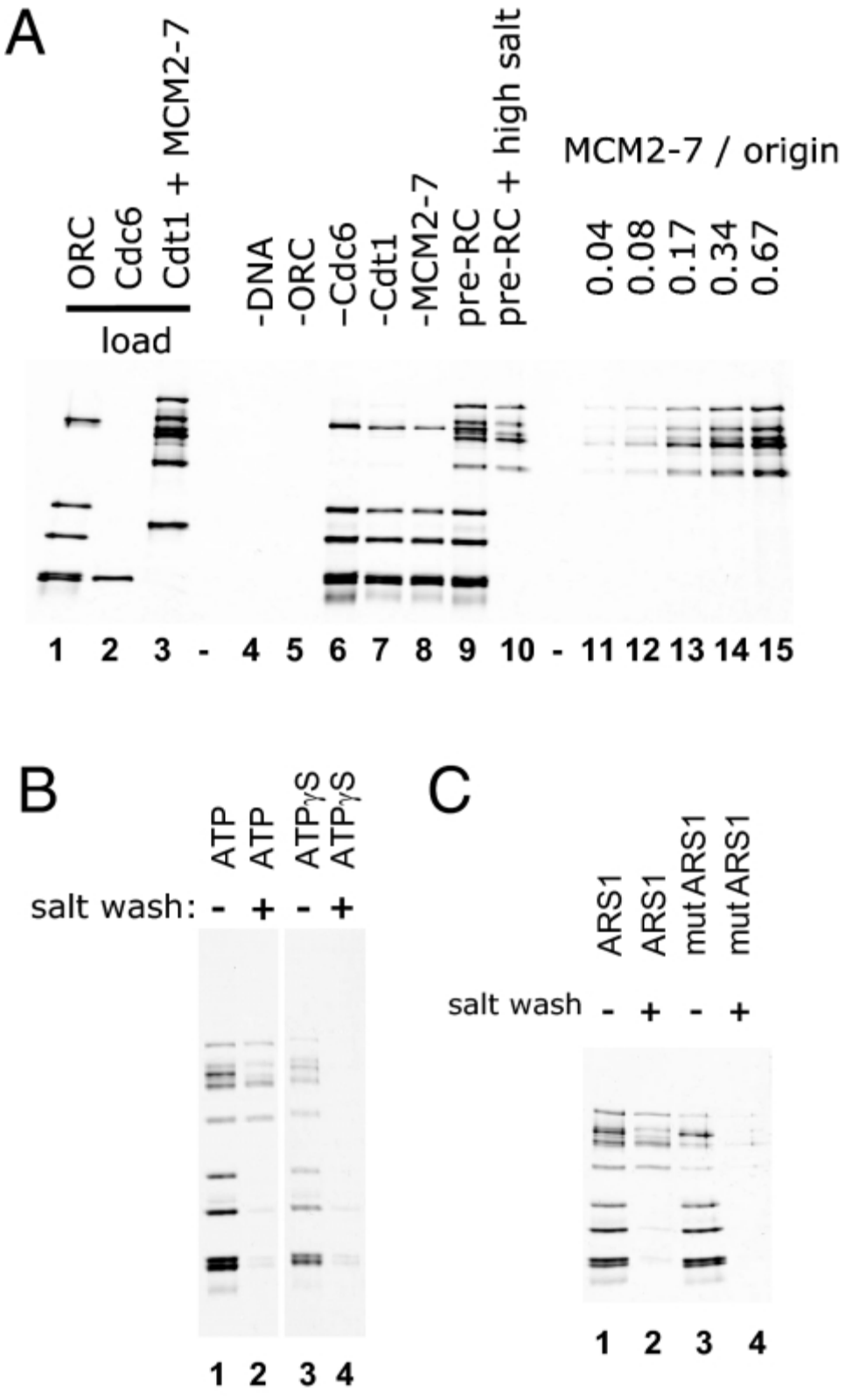

Figure 2. In vitro reconstitution of pre-RC formation. (*A*) Loading of MCM2-7 is dependent on ORC, Cdc6, Cdt1, and DNA. Pre-RC assembly was performed with 6 nM pUC19ARS1, 40 nM ORC, 80 nM Cdc6, 40 nM Cdt1, and 40 nM MCM2-7. Lanes 1–3: 10% load of each protein used in the reaction. Lanes 4–8: 1 component was absent from the reaction: DNA, ORC, Cdc6, Cdt1, or MCM2-7. Complete pre-RC reaction (lane 9) and salt-extracted pre-RC reaction (lane 10). Lanes 11–15: quantification of the number of hexameric MCM2-7 per origin DNA. (*B*) In vitro pre-RC formation is ATP dependent. The

reactions were carried out as in *A* with ATP (lanes 1 and 2) or with the nonhydrolyzable ATP analogue ATPγS (lanes 3 and 4). (*C*) In vitro pre-RC formation is sequence specific. The reactions were carried out as in *A* with a WT ARS1 (lanes 1 and 2) or with mutant DNA (A- B2- B3-) (lanes 3 and 4).

A hallmark of successful loading of MCM2-7 is that the complex becomes resistant to high salt (7, 8, 12, 24, 25). MCM2-7 bound to DNA via ORC-Cdc6-mediated protein–protein interactions becomes destabilized during the high-salt wash and consequently removed, but successfully loaded MCM2-7 is salt resistant. We use the nomenclature (bound vs. loaded) to distinguish between these 2 different types of association.

When the pre-RC reaction was challenged with high salt (Fig. 2A, lane 10) we identified salt-resistant MCM2-7 associated with DNA (12). Approximately half of the MCM2–7 complexes were removed by salt extraction, which is similar to previous observations (7, 8). We quantified the amount of loaded MCM2-7 by comparing the salt-resistant MCM2-7 toward an MCM2-7 dilution series and observed approximately 0.2 hexamers per DNA. This was a significant improvement in efficiency; we estimated at least a 50-fold increase in MCM2-7 loading compared with a previous report (25).

The MCM2-7 loading was dependent on ATP hydrolysis (Fig. 2B). MCM2-7 complexes that associated with the origin DNA in the presence of ATPγS were entirely removed from the DNA by salt extraction. A mutant ARS1 DNA, carrying mutations in the conserved A, B2, and B3 elements, produced significantly reduced MCM2-7 binding and loading in the pre-RC assay compared with WT ARS1 DNA (Fig. 2C), which indicates sequence-specific loading of MCM2-7 on origin DNA. These data are consistent with results from other reconstituted pre-RC systems from Xenopus (26) and yeast (25), and other whole extract based pre-RC reactions from yeast (5, 7, 8, 24). But our pre-RC assay was significantly more efficient in MCM2-7 loading than previously observed.

Loaded MCM2-7 Can Slide Off Linear DNA but Not Circular DNA. It has been hypothesized that loaded MCM2-7 is salt resistant because it forms a ring around DNA (7, 8, 12, 24). To test the idea directly, we asked whether loaded MCM2-7 could slide on dsDNA. A ring-shaped complex should be able to slide and fall off the end of a linear DNA molecule. However, if both ends of the DNA were blocked by streptavidin, the ring should be prevented from falling off and remain associated with DNA. We used linear DNA fragments containing an origin in the center, which were blocked at either one or both ends with streptavidin, and compared them with a circular plasmid. The binding of MCM2-7 to the differently blocked 1-kb DNA fragments and a plasmid control was comparable (Fig. 3, lanes 1–4). All pre-RC factors apart from loaded MCM2-7 were removed using high salt, and MCM2-7 was recovered on the circular DNA as expected but was only found on linear DNA when both ends were blocked with streptavidin (Fig. 3, lanes 5–8). This result shows that MCM2-7 can slide on DNA in either direction, because blocking a single end of the DNA molecule did not result in MCM2-7 accumulation. Sliding of MCM2-7 is consistent with the idea that MCM2-7 encircles DNA.

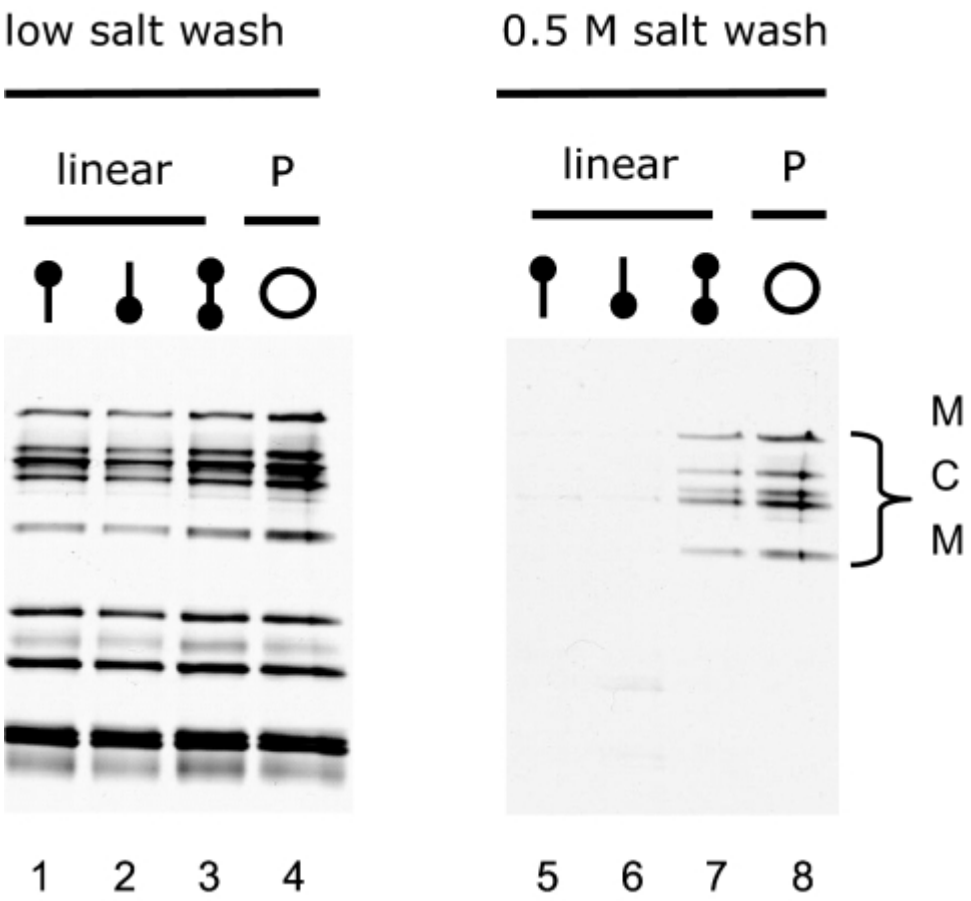

Figure 3. MCM2-7 can slide off DNA ends. The reactions were carried out as in Fig. 2*A*, but 4 different DNA variants were used. As indicated in the figure, linear ARS1 fragments with either one end (lanes 1, 2, 5, and 6) or both ends (lanes 3 and 7) blocked with streptavidin and a circular plasmid pUC19ARS1 (lanes 4 and 8) were used. Salt washes are indicated. MCM2-7 was only retained on linear DNA when both ends were blocked.

MCM2-7 Forms a Double Hexamer on DNA. The structure and organization of the replicative helicase from eukaryotes, MCM2-7, in the presence and absence of DNA is not known but has important implications for helicase loading and pre-IC formation. We started addressing these questions by analyzing the size of MCM2-7 before loading and MCM2-7 after loading onto DNA by gel filtration (Fig. 4). Using the in vitro pre-RC assay we loaded MCM2-7 onto DNA, washed the complex with high salt to select for loaded MCM2-7, and released the complex from DNA using very high concentrations of DNase I, which ensured complete digestion of the DNA. This reaction represents MCM2-7 after loading. In a control reaction, MCM2-7 was mixed with DNA in the absence of other pre-RC proteins and then incubated with DNase I (Fig. 4A). This latter reaction represents MCM2-7 before loading. Both reactions were fractionated on a calibrated gel-filtration column (Fig. 4C), and the elution profile of MCM2-7 was analyzed by immunoblotting with an anti-Mcm2 antibody. MCM2-7 before loading (Fig. 4A) fractionated at 669 kDa, consistent with the calculated mass of 605 kDa for MCM2-7. However, MCM2-7 after loading fractionated at a much larger apparent mass of 1,338 kDa (Fig. 4B), consistent with the 1,210 kDa calculated molecular mass of a double hexamer (Fig. 4B). The experiment suggests that MCM2-7 formed a single hexamer before loading but that during pre-RC formation MCM2-7 assembled into a double hexamer.

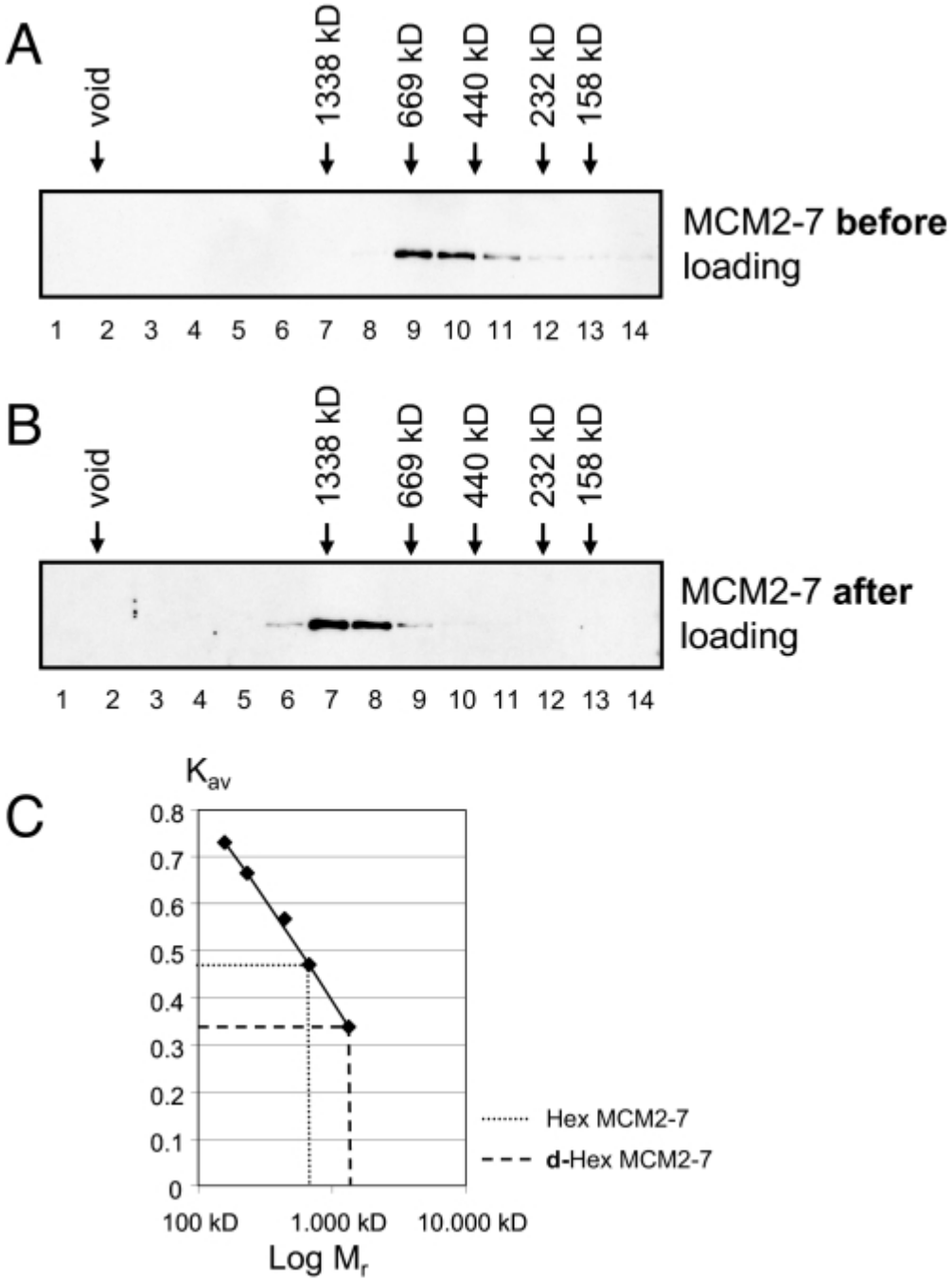

Figure 4. Gel filtration analysis of the oligomerization state of MCM2-7 before and after loading onto DNA. (*A*) MCM2-7 is a single hexamer in solution. MCM2-7 was incubated with DNA and treated with DNase I (see *Materials and Methods*). The sample was separated on a Superose 6 column. Fractions (lanes 1–14) were separated by 7.5% SDS-PAGE and analyzed by Western blotting using an anti-Mcm2 antibody. (*B*) MCM2-7 forms a double hexamer in the pre-RC. Reactions were prepared as described in Fig. 2*A* (lane 10). DNase I mediated release of the protein–DNA complexes, and analyses were done as in *A*. (*C*) Calibration of a Superose 6 column. The marker proteins used are described in *Materials and Methods*. The *x* axis was plotted as the log of the molecular weight in kDa and the *y* axis as the K_{av} value [K_{av} = (Ve − Vo)/(Vt − Vo)] according to the manufacturer's instructions.

EM Observation of the Single and Double MCM2-7 Hexamer. MCM2-7 double hexamer formation should lead to a significant change in size and shape when compared with the single hexamer. To

study this structural change we compared “MCM2-7 before loading” with salt-washed “MCM2-7 after loading” in the electron microscope (Fig. 5). The pre-RC reaction was assembled in solution and then treated with high salt to dissociate all pre-RC proteins from the DNA apart from loaded MCM2-7, which is salt stable. All free proteins were subsequently removed by gel-filtration, and the purified loaded MCM2-7–DNA complex was studied with negative stain EM. Fig. 5A shows MCM2-7 single hexamers before loading. The complex was round or barrel shaped depending on the viewing angle, and we measured an average diameter of 13 nm. This was in stark contrast to MCM2-7 after loading, which was significantly bigger (Fig. 5B and Fig. S1). The loaded MCM2-7 measured 25 nm by 16 nm and was approximately twice the size of MCM2-7 before loading. The shape also changed significantly: the molecule was more elongated, and the ring structures originating from the ATPase and zinc finger domains were noticeable. The architecture of the loaded MCM2-7 resembled the double hexamer found in MCM of archaea (27) and simian virus 40 (SV40) T-antigen (28), consistent with our biochemical sizing analysis.

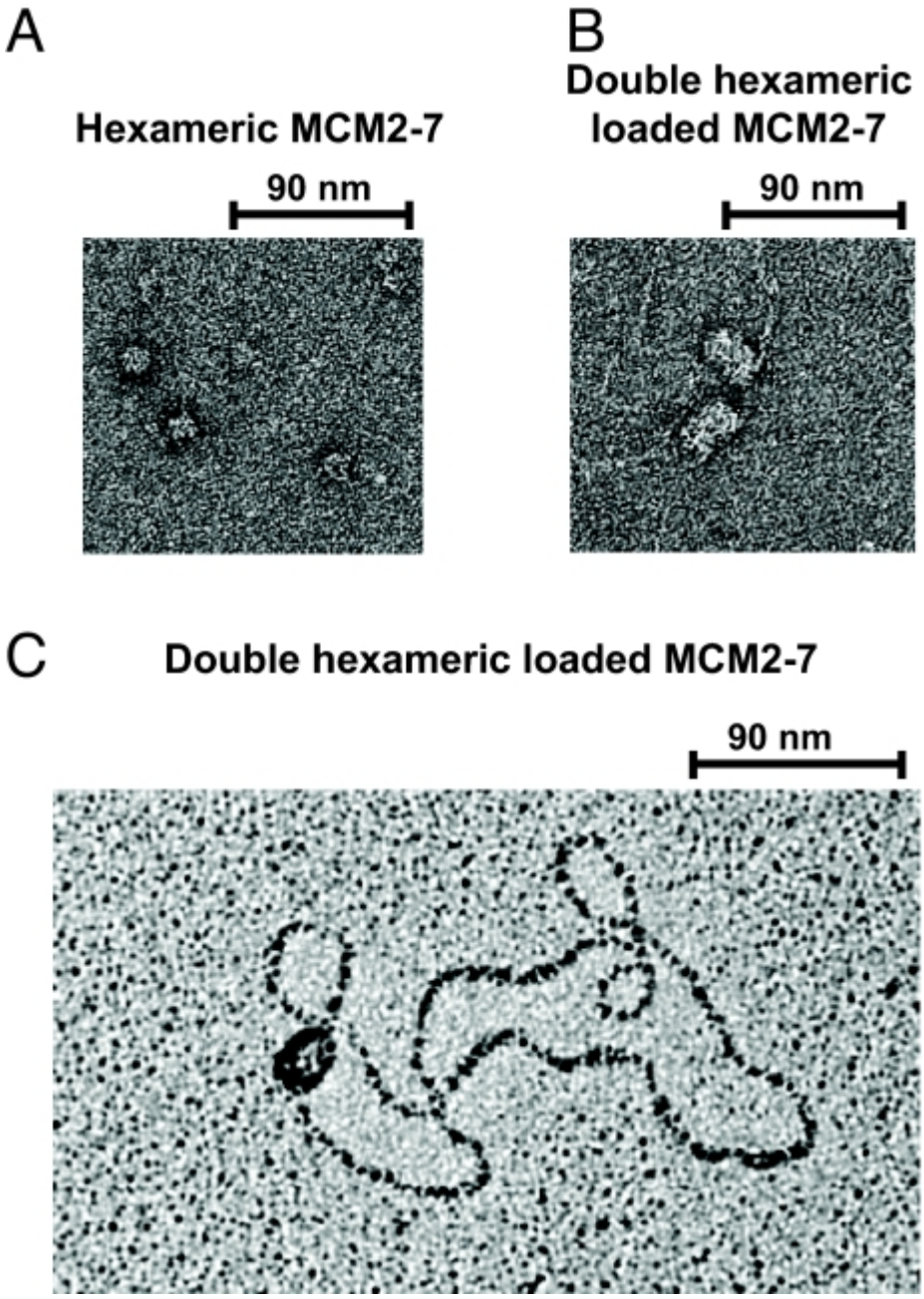

Figure 5. EM analysis of MCM2-7 before and after loading. (*A*) MCM2-7 before loading. MCM2-7 was diluted in ATPγS-containing buffer and visualized by negative staining with uranyl acetate. (*B*) Salt-washed MCM2-7 after loading. Samples were prepared as described in *Materials and Methods*. The protein–DNA complexes were stained as in Fig. 5*A*. (*C*) Salt-washed MCM2-7 after loading. Samples were prepared as described in Fig. 5*B* but visualized by rotary shadowing with platinum; dsDNA seems to pass through the center of a ring-shaped MCM2-7 complex.

To visualize the path of DNA through the MCM2-7 complex, we used a platinum shadowing technique (29). For this method the DNA-bound complex was adsorbed to a mica surface and rotary shadowed with platinum, which produces a high contrast in the EM. In the micrograph, the circular DNA and loaded MCM2-7 were clearly visible, and the DNA seemed to pass through the center of the MCM2-7 complex (Fig. 5C and Figs. S2 and S3). The loaded MCM2-7 complexes displayed an oval shape, as expected for an MCM2-7 double hexamer (30). The mica adsorption technique used here does not allow the visualization of ssDNA (29). The strong contrasts of the DNA molecules in our micrographs (Fig. 5C) imply that a double hexamer MCM2-7 is loaded on dsDNA.

Discussion

In the present study, we found that the eukaryotic replicative MCM2-7 helicase forms a hexamer in the absence of DNA, but during pre-RC formation the complex assembles into a double hexamer.

MCM2-7 Helicase Structure in Solution. MCM2-7 can assume different oligomeric states, which have been observed in previous MCM2-7 purifications and yielded complexes of divergent size and composition, including monomers, hexamers, and larger oligomers (17, 20, 21). The purified MCM2-7 from G1 arrested yeast was a single hexameric complex as judged by its size and shape. All 6 subunits were present in stoichiometric amounts. This result is consistent with the organization of the replicative helicases in bacteria, papillomavirus, and SV40 (1). Archaeal MCMs vary between species and form both hexameric and double-hexameric complexes in solution (27). However, how archaeal MCM is loaded onto DNA is currently unclear.

In Vitro Reconstitution of Pre-RC Formation with Recombinant ORC, Cdc6, Cdt1, and Purified MCM2-7. Eukaryotic helicase loading has been reconstituted using purified protein from Xenopus (26) and from yeast (25). The use of recombinant ORC, Cdc6, and Cdt1 together with highly purified and structurally well-defined MCM2-7 from yeast yielded a very efficient reaction to study pre-RC formation. This reconstituted reaction reflects the in vivo dependencies of pre-RC formation: a requirement for all pre-RC proteins, hydrolyzable ATP, and origin DNA (4, 5, 7, 8, 12, 31, 32).

MCM2-7 Forms a Ring-Shaped Double Hexamer on DNA. The data suggest that the MCM2-7 complex exists as a single hexamer that binds to Cdt1 and is then loaded onto the origin DNA by ORC and Cdc6. The end product contains a linked, double MCM hexamer loaded onto dsDNA, which we

showed by EM and biochemical analyses. Theoretically, one could argue that MCM2-7 could be bound to ssDNA, because a single strand of DNA could pass on the outside of the double hexamer. Sliding should therefore promote DNA unwinding, but ssDNA cannot be detected at replication origins during G1, and we did not detect ssDNA during pre-RC formation. Therefore, the data are best explained by MCM2-7 encircling and sliding on dsDNA.

Our data indicate that the loaded MCM2-7 complex can slide on DNA, but what is the function of MCM2-7 sliding? During G1 5–10 double-hexameric MCM2-7 complexes are loaded onto DNA (9). Sliding could be important to enable repetitive loading of MCM2-7, where 1 loaded complex needs to slide away, making space for loading of a second complex. During pre-IC formation it is likely that only 1 double hexamer is activated, and the additional MCM complexes probably slide ahead of the replication fork. These sliding MCMs may be necessary to reestablish new replication forks when a fork collapses owing to DNA damage (10, 11).

The observation that a double hexamer of MCM2-7 is loaded coordinately on to origin DNA raises the question of how ORC and Cdc6 orchestrate this reaction. S. cerevisiae MCM2-7 and Cdt1 form a complex (6), and initial binding of this complex to ORC-Cdc6-DNA during G1 is independent of ATP hydrolysis (7, 8, 24). This suggests that the heptamer of ORC-Cdc6 on origin DNA represents a landing pad for the heptameric Cdt1-MCM2-7 complex. The ORC-Cdc6 complex adopts a ring-like structure that has a diameter similar to the diameter of the MCM2-7 hexamer ring (4). But how could double hexamer formation be achieved? It is possible that once the first MCM2-7 complex is bound to ORC-Cdc6-DNA a second MCM2-7 hexamer could bind before the 2 MCM2-7 hexamers are loaded together on DNA. An alternative possibility is that there are multiple ORC-Cdc6 complexes at each origin. ORC binds to DNA in a directional manner dependent on the A and B1 origin DNA elements, but there is the potential for another ORC to bind to the B2 element in the opposite direction that could load a second MCM2-7 (2, 33).

It is also unclear how the preloaded MCM2-7 hexamer is opened so that it can topologically link to dsDNA. It is possible that ATP hydrolysis by ORC and Cdc6 could be necessary to open the MCM2-7 ring structure. This seems likely because ORC and Cdc6 share some similarity with the RFC–clamp loader complex, which opens the PCNA ring and loads PCNA onto DNA (4, 12).

Helicase loading onto DNA has been reconstituted in bacteria and virus DNA replication reactions. In bacteria, origin DNA is initially unwound by DnaA, which promotes the DnaA- and DnaC-assisted loading of 2 single hexameric DnaB helicase complexes onto ssDNA (34). Large T-antigen, the replicative helicase from SV40, forms a hexamer in solution. During DNA loading T-antigen initially unwinds the DNA, and a T-antigen double hexamer is formed on ssDNA (35). The related E1 helicase is established via transient formation of 2 trimers of E1 on the origin DNA that morph into a double hexamer and locally unwinds DNA at the origin (36). In both bacteria and virus DNA replication, the loaded complexes are immediately active as helicases. This is a major difference from DNA

unwinding at eukaryotic cell origins, where the loaded MCM2-7 needs further activation by kinases and other protein factors to perform as a Cdc45, MCM2-7, GINS (CMG) helicase (19).

A Role for MCM Double Hexamers to Establish Bidirectional Replication Forks. The generation of a double-hexameric MCM2-7 complex is clearly an advantage for the cell, because this enables simultaneous activation of 2 single hexameric helicases during pre-IC formation, which would represent a straightforward mechanism to establish bidirectional DNA replication forks. The 2 hexamers within the MCM2-7 double hexamer are very likely linked to each other via their N-termini, on the basis of the fact that the archaeal MCM N-termini bind directly to each other, as observed in biochemical experiments and a crystal structure (30, 37). During pre-IC formation it is possible that the double hexamer splits to form 2 active forks enabling bidirectional replication (Fig. 6B Left and Center). On the basis of the similarities between the papillomavirus E1 helicase and MCM2-7, we suggest that pre-IC proteins promote reopening of the MCM2-7 hexamer and exclusion of a single strand from the MCM2-7 complex. This would allow the CMG helicase unwinding DNA following the steric exclusion model (19, 38) (Fig. 6B Left). An alternative ploughshare model predicts the presence of a pin in the center of the MCM2-7 complex that separates the 2 strands of DNA (39) (Fig. 6B Center). A third model, based on studies with T-antigen, suggests that the double-hexameric complex is maintained. Here, DNA is pumped into the center of the complex, and ssDNA leaves at the interface between the 2 hexamers through specific channels (28) (Fig. 6B Right). Regardless of the exact helicase mechanism, the formation of the MCM2-7 double hexamers via their N-termini creates a pair of MCM2-7 helicases in the correct orientation to lay the foundation for bidirectional replication forks. MCM2-7 from yeast has been isolated from a replication fork as part of the replisome progression complex (40). Quantitative Western blotting suggested that MCM2-7 was present as a single hexamer within the replisome progression complex. However, these complexes were isolated from hydroxyurea arrested cells, which could potentially disrupt double hexamers, because hydroxyurea promotes uncoupling of the MCM helicase from the DNA polymerase. As such, it is currently unclear whether MCM2-7 exists as a single hexamer or double hexamer at the replication fork in vivo. The 3 proposed models for MCM2-7 helicase activity shown in Fig. 6B are attractive and testable upon addition of extracts from S-phase cells to the pre-RC formed in vitro. It will be challenging but very interesting to decipher the organization of the MCM2-7 helicase at the replication fork and its unwinding mechanism.

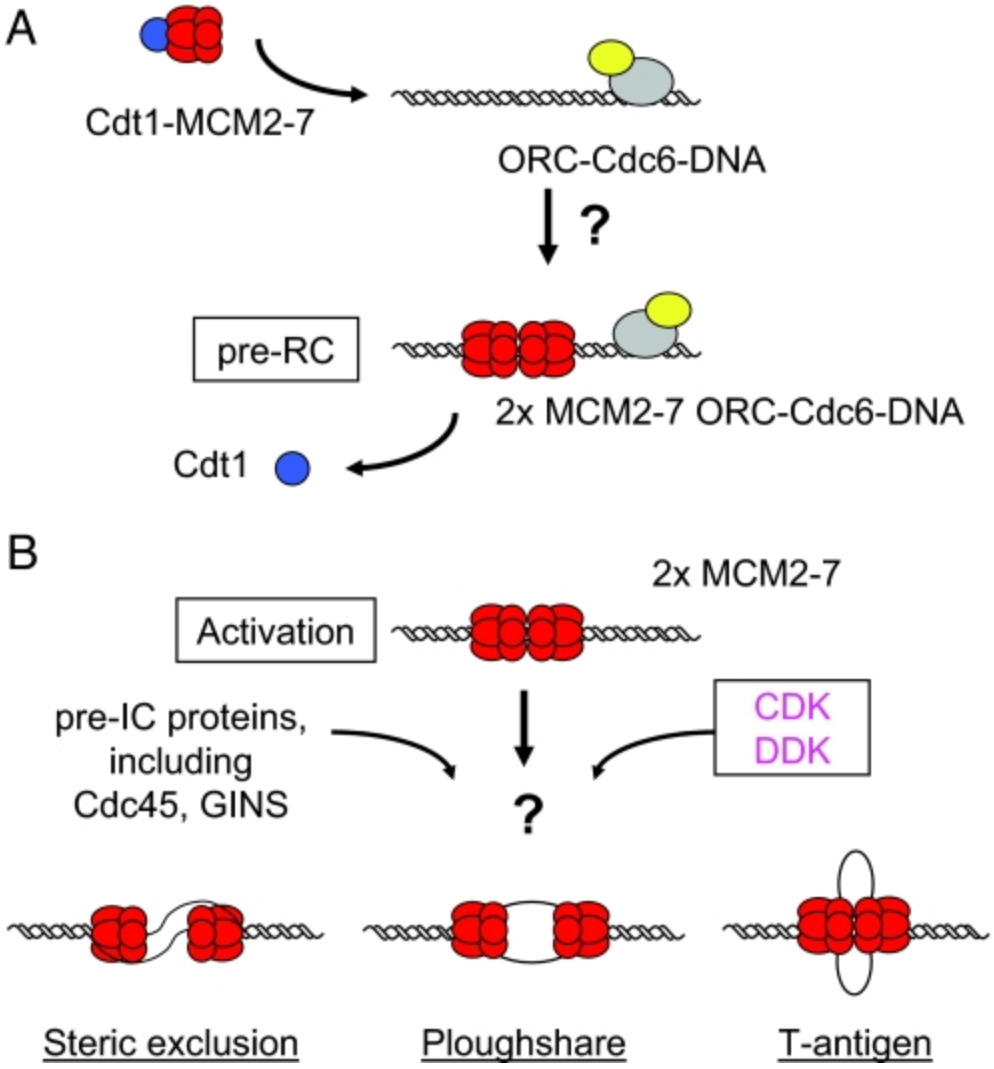

Figure 6. Speculative model of MCM2-7 loading and activation. (*A*) During pre-RC formation ORC-Cdc6-DNA is joined by a Cdt1-MCM2-7 complex. The reaction is dependent on all pre-RC protein factors and ATP hydrolysis, but it is currently not known how double-hexameric MCM2-7 assembles at an origin. (*B*) During pre-IC formation double-hexameric MCM2-7 is activated by kinases and proteins; exact roles of each are unknown. Three models for potential helicase activity at the replication fork are shown. The model on the left suggests that 1 ssDNA strand passes inside the MCM2-7 hexamer to drive movement similar to the papillomavirus E1 helicase (38); the middle model predicts a separation of the MCM2-7 double hexamer with dsDNA through its middle and is commonly referred to as the ploughshare model (39). The model on the right is similar to a proposed SV40 T-antigen DNA unwinding model (28), whereby the double hexamer pumps dsDNA toward the center and ssDNA exits through pores within the middle of the complex.

Materials and Methods

Plasmids, Oligonucleotides, and Strains. pUC19ARS1 was prepared by cloning an EcoRI-HindIII fragment of pARS1 WTA (4) into pUC19. The mutant pUC19ARS1 was cloned in the same way from the pARS1A- B2-, B3- mutant (4). The 1-kb ARS1 fragment was amplified by PCR using pUC19ARS1 as template and the primer combination listing in Table S1. Sequences of oligonucleotides used for the

cloning of the 6 MCM2-7 subunits and Cdt1 are listed in Table S1. The AS499 (MATa bar1Δ leu2–3,112 ura3–52 his3-Δ200 trp1-Δ63 ade2–1 lys2–801 pep4) yeast strain was a gift from Luis Aragon.

Purification of ORC, Cdc6, and Cdt1. The ORC and Cdc6 proteins were prepared as described previously (4). Cdt1 was cloned as a GST fusion protein (GST-Cd1) and expressed as described previously (4). The fusion protein was bound to glutathione agarose (Sigma) in buffer T [50 mM Tris-HCl (pH 7.2), 150 mM NaCl, 5 mM MgCl2, 1 mM DTT, and 1% Triton] at 4 °C for 2 h, and then the GST tag was cleaved by addition of 240 U of PreScission Protease (GE Healthcare). The eluate was diluted with 1 volume buffer D [25 mM Hepes (pH 6.0), 5 mM MgCl2, and 1 mM DTT] and bound to SP Sepharose (GE Healthcare). Cdt1 was eluted with buffer E [25 mM Tris-Hl (pH 7.2), 25 mM Hepes-KOH pH 6.0, 250 mM NaCl, 5 mM MgCl2, 1 mM DTT, 0.1% Triton, and 15% glycerol] and applied to a Sephacryl 200 16/60 column (GE Healthcare) preequilibrated with buffer E. Peak fractions were concentrated and stored at −80 °C. One liter of bacteria culture yielded approximately 0.23 mg of pure Cdt1 with a concentration of 0.4 mg/mL.

Cloning and Purification of MCM2-7. Untagged Mcm2, 4–7, and N-terminal HA-tagged Mcm3 subunits were cloned into pESC yeast epitope tagging vectors (Stratagene). The 3 resulting plasmids, pESC-Leu-Mcm2-Mcm7 (p14), pESC-Trp-Mcm4-Mcm6 (p15), and pESC-Ura-HA-Mcm3-Mcm5 (p232) were transformed in strain AS499 (Table S2). The proteins were expressed as described previously, with minor modifications (41). After the addition of galactose the 2-L culture (OD 1.8) was arrested with alpha factor (2.5 μg/mL) for 3 h. The cells were lysed in a freezer mill, resuspended in buffer M [25 mM Hepes-KOH, 300 mM potassium glutamate (KGlu), 10 mM MgAc, 50 μM zinc acetate (ZnAc), 10% glycerol, and 0.1% Triton] plus complete protease inhibitor (Roche) and centrifuged at 27,600 × g for 1 h at 4 °C. The supernatant was incubated with 1.5 mL of HA beads for 2 h at 4 °C and washed twice with buffer M plus 3 mM ATP and protease inhibitors. The protein was eluted by the addition of HA peptide 0.5 mg/mL in buffer M plus 3 mM ATP. Eluted protein was applied to a Superdex 200 16/60 column (GE Healthcare) preequilibrated with buffer M plus 0.1 mM ATP. The fractions containing MCM2-7 were concentrated and stored at −80 °C. A standard 2-L culture yielded approximately 0.24 mg of pure MCM2-7 protein at a concentration of 0.8 mg/mL.

In Vitro Pre-RC Assembly Assay. Pre-RCs were assembled in a 2-step reaction. Fifty microliters of load 1 containing 40 nM ORC, 80 nM Cdc6, and 120 U Lambda phosphatase in buffer A [25 mM Hepes-KOH (pH 7.5), 100 mM KGlu, 10 mM MgAc, 50 μM ZnAc, 3 mM ATP, 5 mM DTT, 0.1% Triton, and 5% glycerol] plus 2 mM MnCl2 was added to 6 nM pUC19-ARS1 plasmid beads (see SI Methods) and 18 nM linear ARS1 fragments beads for 15 min at 24 °C. Beads were washed 3 times with buffer A plus 1 mM EDTA to remove nonbound proteins. Fifty microliters of load 2 containing 40 nM Cdt1 and 40 nM MCM2-7 preincubated for 10 min at 24 °C in buffer A was added to the beads and incubated for 15 min at 24 °C. Beads were washed 3 times with either buffer A plus 0.5 mM EDTA or buffer A plus 0.5 mM EDTA and 500 mM NaCl without KGlu before digestion with 1 U of DNase I in buffer A plus 5 mM CaCl2 for 6 min at 24 °C. For the experiment described in Fig. 2C a 132 molar excess of a 291 bp ARS1 fragment was added to the ORC-Cdc6-DNA complexes as competitor (42).

Gel Filtration Analysis. Proteins were fractionated on a Superose 6 column in buffer B [25 mM Hepes-KOH (pH 7.5), 75 mM NaCl, 5 mM MgCl2, 0.1% Triton, 10% glycerol, 100 µM EDTA, and 100 µM ZnAc]. Five reactions were prepared as described for the in vitro pre-RC assembly assay, combined, and loaded onto a Superose 6 column. For the MCM2-7 sample "before loading," ORC, Cdc6, and Cdt1 were omitted. The following standards calibrated the column: thyroglobulin tetramer (1,338 kDa), thyroglobulin dimer (669 kDa), ferritin (440 kDa), catalase (232 kDa), and aldolase (158 kDa).

Electron Microscopy. Samples were prepared as described for the in vitro pre-RC assembly assay, but DNA was not coupled to the beads. For the high-salt wash 500 mM NaCl was added directly to the sample and incubated for 5 min. The mixture was centrifuged for 2 min at 18,600 × g at 4 °C and loaded onto a Sephacryl 400 MicroSpin column (700 µL, 75% slurry), preequilibrated with 25 mM Hepes-KOH (pH 7.5), 500 mM NaCl, and 10 mM MgCl2. The column was centrifuged for 5 min at 700 × g, and the sample was diluted 1:10 in 10 mM Tris (pH 7.5) and 10 mM Mg Cl2. For EM analysis the sample was adsorbed to freshly cleaved mica and rotary shadowed with platinum vapor (29). Negative stain with 2% uranyl acetate was performed as described previously (43).

Acknowledgments.

We thank Niall Dillon, Matthias Merkenschlager, Ana Pombo, and members of the DNA Replication Group for helpful comments on the manuscript; and Luis Aragon for yeast strains. This work was supported by the United Kingdom Medical Research Council (C.S.), National Institutes of Health (NIH) Grant GM45436 (to B.S.), the Goldring Family Foundation (B.S.), NIH Grant GM74985 (to H.L.), and by Brookhaven National Laboratory Laboratory Directed Research and Development project number 06–06 (to H.L.).

References

1. Stillman B. Origin recognition and the chromosome cycle. FEBS Lett. 2005;579:877–884.

2. Bell SP, Stillman B. ATP-dependent recognition of eukaryotic origins of DNA replication by a multiprotein complex. Nature. 1992;357:128–134.

3. Diffley JF, Cocker JH, Dowell SJ, Rowley A. Two steps in the assembly of complexes at yeast replication origins in vivo. Cell. 1994;78:303–316.

4. Speck C, Chen Z, Li H, Stillman B. ATPase-dependent cooperative binding of ORC and Cdc6 to origin DNA. Nat Struct Mol Biol. 2005;12:965–971.

5. Chen S, de Vries MA, Bell SP. Orc6 is required for dynamic recruitment of Cdt1 during repeated Mcm2–7 loading. Genes Dev. 2007;21:2897–2907.

6. Tanaka S, Diffley JF. Interdependent nuclear accumulation of budding yeast Cdt1 and Mcm2–7 during G1 phase. Nat Cell Biol. 2002;4:198–207.

7. Bowers JL, Randell JC, Chen S, Bell SP. ATP hydrolysis by ORC catalyzes reiterative Mcm2–7 assembly at a defined origin of replication. Mol Cell. 2004;16:967–978.

8. Randell JC, Bowers JL, Rodriguez HK, Bell SP. Sequential ATP hydrolysis by Cdc6 and ORC directs loading of the Mcm2–7 helicase. Mol Cell. 2006;21:29–39.

9. Laskey RA, Madine MA. A rotary pumping model for helicase function of MCM proteins at a distance from replication forks. EMBO Rep. 2003;4:26–30.

10. Ge XQ, Jackson DA, Blow JJ. Dormant origins licensed by excess Mcm2–7 are required for human cells to survive replicative stress. Genes Dev. 2007;21:3331–3341.

11. Ibarra A, Schwob E, Mendez J. Excess MCM proteins protect human cells from replicative stress by licensing backup origins of replication. Proc Natl Acad Sci USA. 2008;105:8956–8961.

12. Donovan S, Harwood J, Drury LS, Diffley JF. Cdc6p-dependent loading of Mcm proteins onto pre-replicative chromatin in budding yeast. Proc Natl Acad Sci USA. 1997;94:5611–5616.

13. Zou L, Stillman B. Formation of a preinitiation complex by S-phase cyclin CDK-dependent loading of Cdc45p onto chromatin. Science. 1998;280:593–596.

14. Sclafani RA, Holzen TM. Cell cycle regulation of DNA replication. Annu Rev Genet. 2007;41:237–280.

15. Clarey MG, et al. Nucleotide-dependent conformational changes in the DnaA-like core of the origin recognition complex. Nat Struct Mol Biol. 2006;13:684–690.

16. Perkins G, Diffley JF. Nucleotide-dependent prereplicative complex assembly by Cdc6p, a homolog of eukaryotic and prokaryotic clamp-loaders. Mol Cell. 1998;2:23–32.

17. Bochman ML, Schwacha A. The Mcm2–7 complex has in vitro helicase activity. Mol Cell. 2008;31:287–293.

18. Labib K, Tercero JA, Diffley JF. Uninterrupted MCM2-7 function required for DNA replication fork progression. Science. 2000;288:1643–1647.

19. Moyer SE, Lewis PW, Botchan MR. Isolation of the Cdc45/Mcm2–7/GINS (CMG) complex, a candidate for the eukaryotic DNA replication fork helicase. Proc Natl Acad Sci USA. 2006;103:10236–10241.

20. Schwacha A, Bell SP. Interactions between two catalytically distinct MCM subgroups are essential for coordinated ATP hydrolysis and DNA replication. Mol Cell. 2001;8:1093–1104.

21. Davey MJ, Indiani C, O'Donnell M. Reconstitution of the Mcm2–7p heterohexamer, subunit arrangement, and ATP site architecture. J Biol Chem. 2003;278:4491–4499.

22. Nguyen VQ, Co C, Li JJ. Cyclin-dependent kinases prevent DNA re-replication through multiple mechanisms. Nature. 2001;411:1068–1073.

23. Forsburg SL. Eukaryotic MCM proteins: Beyond replication initiation. Microbiol Mol Biol Rev. 2004;68:109–131.

24. Seki T, Diffley JF. Stepwise assembly of initiation proteins at budding yeast replication origins in vitro. Proc Natl Acad Sci USA. 2000;97:14115–14120.

25. Kawasaki Y, Kim HD, Kojima A, Seki T, Sugino A. Reconstitution of Saccharomyces cerevisiae prereplicative complex assembly in vitro. Genes Cells. 2006;11:745–756.

26. Gillespie PJ, Li A, Blow JJ. Reconstitution of licensed replication origins on Xenopus sperm nuclei using purified proteins. BMC Biochem. 2001;2:15.

27. Sakakibara N, Kelman LM, Kelman Z. Unwinding the structure and function of the archaeal MCM helicase. Mol Microbiol. 2009;72:286–296.

28. Gomez-Lorenzo MG, et al. Large T antigen on the simian virus 40 origin of replication: A 3D snapshot prior to DNA replication. EMBO J. 2003;22:6205–6213.

29. Spiess E, Lurz R, Mayer F. Electron microscopic analysis of nucleic acids and nucleic acid-protein complexes. In: Mayer F, editor. Methods in Microbiology. Vol 20. London: Academic; 1988. pp. 293–323.

30. Fletcher RJ, et al. The structure and function of MCM from archaeal M. Thermoautotrophicum. Nat Struct Biol. 2003;10:160–167.

31. Liang C, Weinreich M, Stillman B. ORC and Cdc6p interact and determine the frequency of initiation of DNA replication in the genome. Cell. 1995;81:667–676.

32. Cocker JH, Piatti S, Santocanale C, Nasmyth K, Diffley JF. An essential role for the Cdc6 protein in forming the pre-replicative complexes of budding yeast. Nature. 1996;379:180–182.

33. Wilmes GM, Bell SP. The B2 element of the Saccharomyces cerevisiae ARS1 origin of replication requires specific sequences to facilitate pre-RC formation. Proc Natl Acad Sci USA. 2002;99:101–106.

34. Carr KM, Kaguni JM. Stoichiometry of DnaA and DnaB protein in initiation at the Escherichia coli chromosomal origin. J Biol Chem. 2001;276:44919–44925.

35. Mastrangelo IA, et al. ATP-dependent assembly of double hexamers of SV40 T antigen at the viral origin of DNA replication. Nature. 1989;338:658–662.

36. Schuck S, Stenlund A. Assembly of a double hexameric helicase. Mol Cell. 2005;20:377–389.

37. Fletcher RJ, et al. Double hexamer disruption and biochemical activities of Methanobacterium thermoautotrophicum MCM. J Biol Chem. 2005;280:42405–42410.

38. Enemark EJ, Joshua-Tor L. On helicases and other motor proteins. Curr Opin Struct Biol. 2008;18:243–257.

39. Takahashi TS, Wigley DB, Walter JC. Pumps, paradoxes and ploughshares: Mechanism of the MCM2-7 DNA helicase. Trends Biochem Sci. 2005;30:437–444.

40. Gambus A, et al. GINS maintains association of Cdc45 with MCM in replisome progression complexes at eukaryotic DNA replication forks. Nat Cell Biol. 2006;8:358–366.

41. Burgers PM. Overexpression of multisubunit replication factors in yeast. Methods. 1999;18:349–355.

42. Speck C, Stillman B. Cdc6 ATPase activity regulates ORC x Cdc6 stability and the selection of specific DNA sequences as origins of DNA replication. J Biol Chem. 2007;282:11705–11714.

43. Steven AC, et al. Molecular substructure of a viral receptor-recognition protein. The gp17 tail-fiber of bacteriophage T7. J Mol Biol. 1988;200:351–365.